



Journal Name

ARTICLE

Supporting Information

Bimetallic phosphoselenide nanosheets as bifunctional catalysts for 5-hydroxymethylfurfural oxidation and hydrogen evolution

Hao Zhang^{a, b}, Gaocan Qi^{c*}, Wei Liu^{a*}, Shusheng Zhang^d, Qian Liu^e, Jun Luo^f, and Xijun Liu^{b*}

^a Institute for New Energy Materials & Low-Carbon Technologies, School of Materials Science and Engineering, Tianjin University of Technology, Tianjin 300384, China. E-mail: liuweihuludao@163.com

^b State Key Laboratory of Featured Metal Materials and Life-cycle Safety for Composite Structures, School of Resource, Environments and Materials, Guangxi University, Nanning 530004, China. E-mail: xjliu@tjut.edu.cn

^c School of Materials Science and Engineering, Tianjin University of Technology, Tianjin 300384, China. E-mail: gaocanqi@tjut.edu.cn

^d College of Chemistry, Zhengzhou University, Zhengzhou 450000, China.

^e Institute for Advanced Study, Chengdu University, Chengdu 610106, Sichuan, China.

^f ShenSi Lab, Shenzhen Institute for Advanced Study, University of Electronic Science and Technology of China, Longhua District, Shenzhen 518110, China.

Experimental section

Chemicals

All reagents were used directly without further purification as they were analytical grade.

Synthesis of Mn-doped FePSe₃ bulk

Bulk FePSe₃ precursors were obtained through heating catalyst powder in vacuum. Typically, FeCl₂ powder, MnCl₂ powder, selenium powder and phosphorus powder were proportionally enclosed in a quartz ampoule. And then it was vacuum heating at 750 °C for 6 days with a heating rate of 2 °C min⁻¹. After it was cooled to room temperature naturally, the solid powder was washed with carbon disulfide to obtain a series of black Mn-doped FePSe₃ bulk sample. The reference FePSe₃ bulk sample was prepared under the identical synthetic route but without MnCl₂ addition.

Synthesis of Mn-doped FePSe₃ nanosheets

The nanosheets were prepared via an exfoliation process. Specifically, bulk powder (0.1 g) was added into 200 mL of absolute ethylalcohol and then it was exfoliated by ultrasonication for 48 h. After that, the mixed solution was centrifuged, and when the rotation speed was 3000 rpm, the residual bulk sample can be removed; afterwards the remaining sample was centrifuged again at 12,000 rpm. Finally, the moist solid powder was dispersed again in water and lyophilized to get the exfoliated Mn-FePSe₃/NS and FePSe₃/NS.

Material characterizations

The apparent morphology and structure of the materials were characterized using a field emission scanning electron- microscope (SEM) (Nova NanoSEM 450, FEI, USA) and a transmission electron microscope (TEM) (Tecnai G2 F30, FEI, USA). The crystal structure of the materials was characterized using an X-ray diffractometer (XRD) (X'Pert PRO type, PANalytical, Netherlands) in the range of 5° to 80°. Using an x-ray photoelectron spectrometer (XPS) (Thermo Scientific K-Alpha, Shimadzu Kratos) to characterize the surface chemistry of the material (using Al (K α) radiation as a probe). The binding energy was calibrated using the carbon peak (C 1s: 284.8 eV). The chemical structure of the material was tested and analyzed using a Raman spectrometer (LabRAM HR800, Horiba Jobin Yvon, France).

Electrochemical tests

The electrochemical tests were all performed on a CHI760e electrochemical workstation. The catalytic performances of the catalysts were tested with a three-electrode system, in which the studied sample, carbon rod and saturated Hg/HgO were used as working, counter and reference electrode, respectively. Commercial comparison sample preparation: 5 mg 20% Pt/C, 32 μ Nafion, 700 μ L ethanol, and 1 μ L deionized water were mixed, sonicated for 0.5 h, coated with 1 mg cm⁻² on the carbon paper, and dried by iR lamp.

The linear scanning voltammetry (LSV) polarization curves were obtained at a slow sweep rate of 5 mV s^{-1} under $1 \text{ M KOH}/1 \text{ M KOH}+0.5 \text{ M HMF}$. EIS was tested at open circuit voltage and in the frequency range of 0.1 to 100000 Hz. The electrical double layer capacitance (C_{dl}) was calculated from cyclic voltammograms (CV) obtained in the non-Faraday interval ($5 \sim 25 \text{ mV s}^{-1}$) and used to evaluate the electrochemically active specific surface area (ECSA).

The concentration variations of HMF and its oxidation products during the electrolysis were monitored through high-performance liquid chromatography (HPLC, Shimadzu Prominence LC-20AD) on aliquots taken from the electrochemical cells with an ultraviolet-visible detector. $20 \mu\text{L}$ of electrolyte was sampling during potentiostatic electrolysis and diluted to 2 mL with ultrapure water and analyzing it by HPLC. The wavelength of the UV detector was set to 265 nm, mobile phase A and phase B was methanol and 5 mmol L^{-1} ammonium formate aqueous solution, respectively. The ratio of A: B was 3:7 and flow rate was 0.6 mL min^{-1} . A $4.6 \text{ mm} \times 250 \text{ mm}$ Ultimate $5 \mu\text{m}$ AQ-C18 column was used and each separation lasts 10 min.

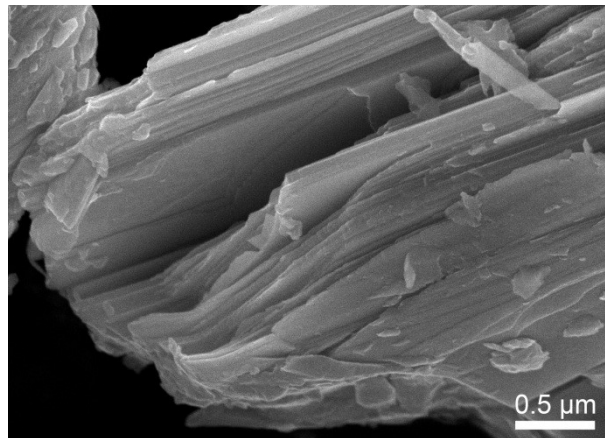


Figure S1. SEM image of the Mn-doped FePSe₃ bulk sample.

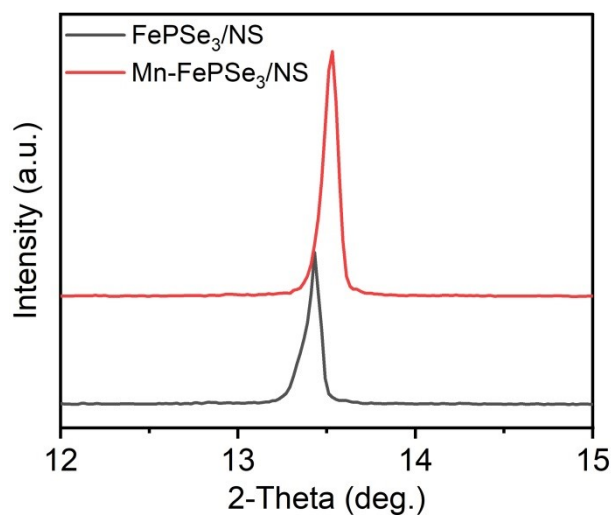


Figure S2. The enlarged XRD patterns of FePSe₃/NS and Mn-FePSe₃/NS.

The ion radius of Mn²⁺ (0.67 Å) is larger than that of Fe²⁺ (0.78 Å), resulting in the lattice constant of FePSe₃ was decreased.

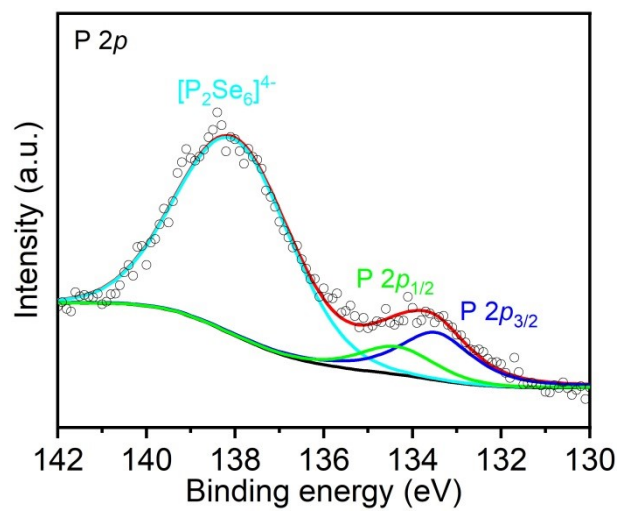


Figure S3. High resolution P 2p XPS spectrum of Mn-FePSe₃/NS.

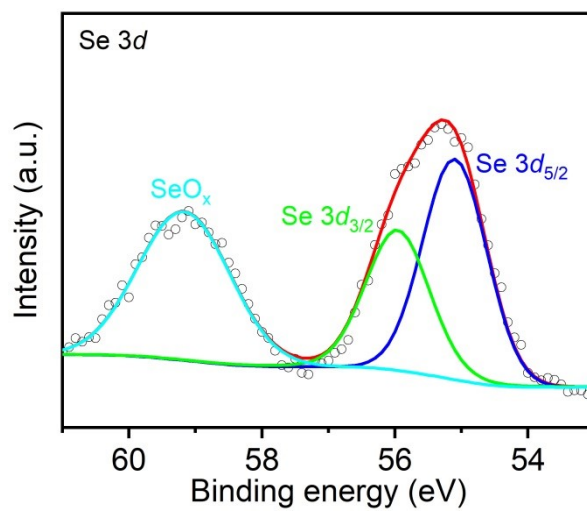


Figure S4. High resolution Se 3d XPS spectrum of Mn-FePSe₃/NS.

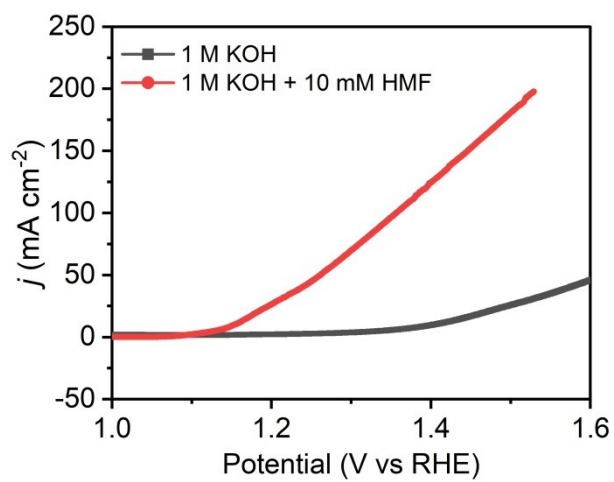


Figure S5. LSV curves of Mn-FePSe₃/NS recorded in different electrolytes.

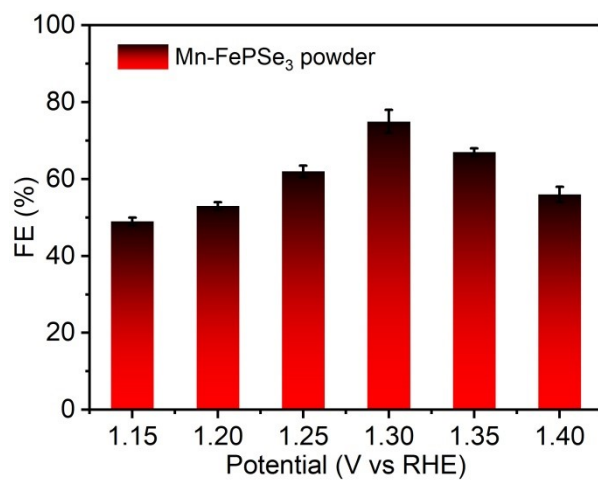


Figure S6. The calculated FE values of Mn-doped FePSe₃ powder.

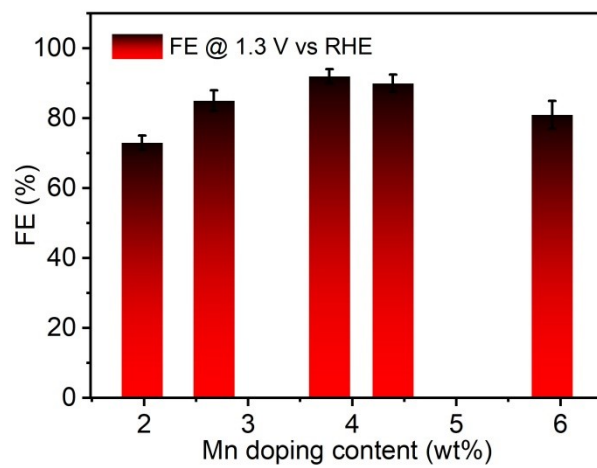


Figure S7. The effect of Mn doping content of Mn-FePSe₃/NS on the HMF oxidation.

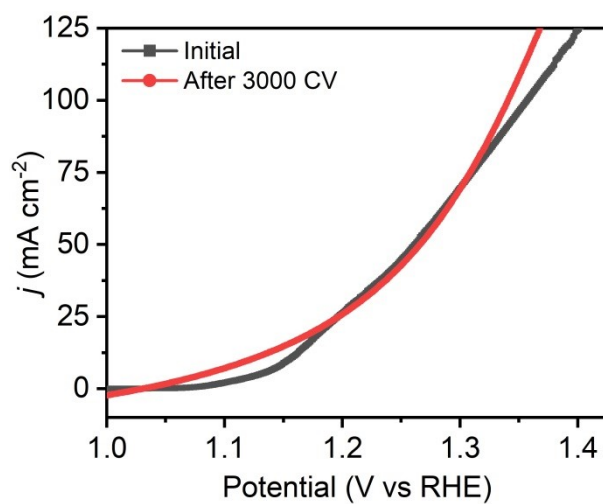


Figure S8. LSV curves of Mn-FePSe₃/NS recorded before and after 3000 cycles.

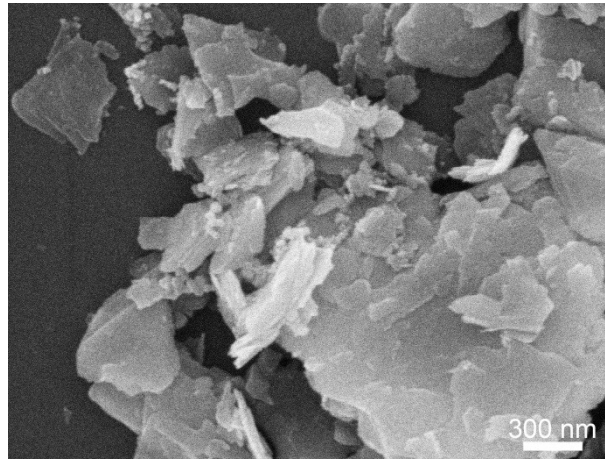


Figure S9. SEM image of Mn-FePSe₃/NS after the electrolysis.

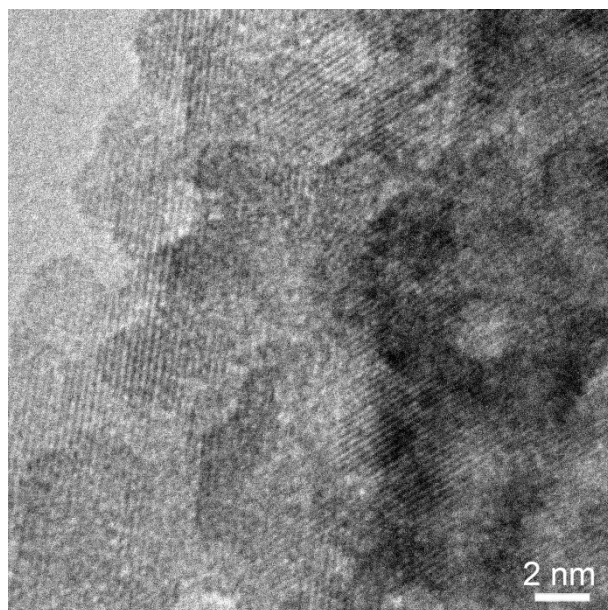


Figure S10. TEM image of Mn-FePSe₃/NS after the electrolysis.

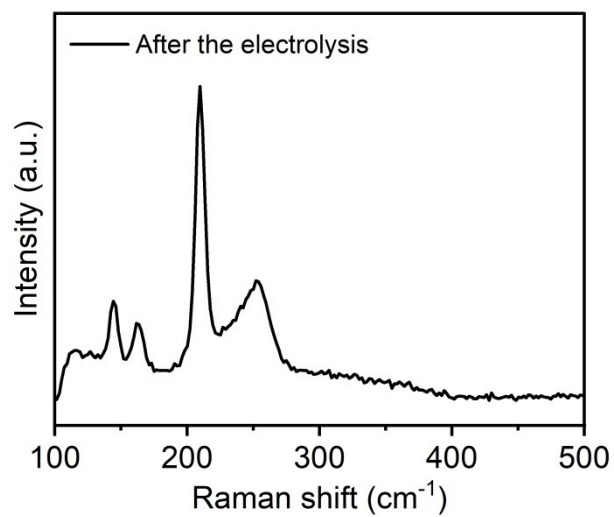


Figure S11. Raman spectrum for Mn-FePSe₃/NS after the electrolysis.

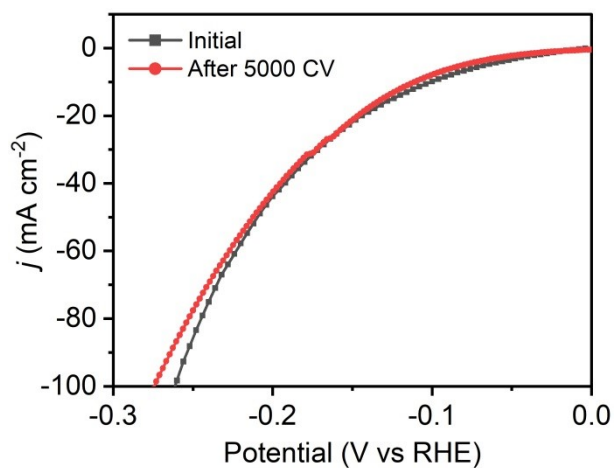


Figure S12. HER LSV curves of Mn-FePSe₃/NS taken before and after 5000 cycles.

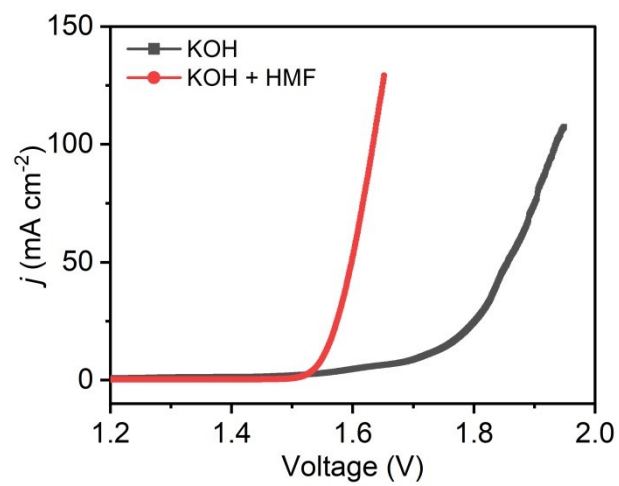


Figure S13. LSV curves recorded in two-electrode system with different electrolytes.

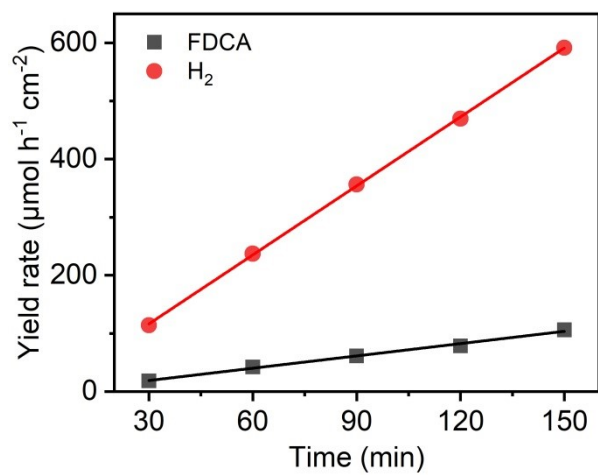


Figure S14. The yield rates of produced FDCA and H_2 achieved on FePSe_3/NS .

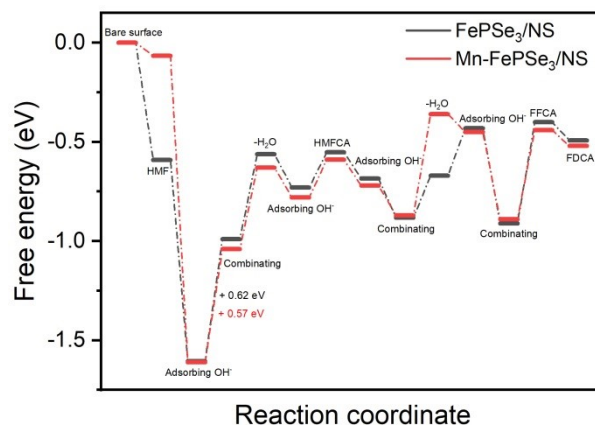


Figure S15. Reaction free energy barrier for the HMF oxidation on FePSe₃/NS (a) and Mn-FePSe₃/NS (b). The free energy barrier of dehydration (that is, potential-determining step) on Mn-FePSe₃/NS is 0.57 eV, smaller than that of FePSe₃/NS (0.62 eV), suggesting the HMF molecule adsorbed on Mn-FePSe₃/NS is more preferential than on FePSe₃/NS to be oxidated to yield FDCA.

Table S1. Comparison of electrocatalytic HER performances of reported catalysts.

Catalysts	Electrolyte	Current density (mA cm ⁻²)	Overpotential @ Current density (mV)	Ref.
Ni–Fe cluster	0.1 M KOH	10	70	<i>Angew. Chem. Int. Ed.</i> 2020 , <i>59</i> , 10934
Ir cluster	1.0 M KOH	10	42.8	<i>Adv. Mater.</i> 2021 , <i>33</i> , 2105400
Ni cluster	1 M KOH	10	17	<i>Energy Environ. Sci.</i> 2021 , <i>14</i> , 3194
Ir cluster	1 M KOH	10	82	<i>Adv. Funct. Mater.</i> 2021 , <i>31</i> , 2101797
single-layer Pt cluster	1 M KOH	5	170	<i>Small</i> 2021 , <i>17</i> , 2100732
Pt cluster	1 M KOH	100	47	<i>Small Struct.</i> 2021 , <i>2</i> , 2100047
Ru cluster	1 M KOH	10	28	<i>Electrochem. Commun.</i> 2019 , <i>101</i> , 23
Cu cluster	1 M KOH	10	134	<i>Adv. Mater.</i> 2017 , <i>29</i> , 1606200
Co cluster	1 M KOH	10	110	<i>Carbon</i> 2020 , <i>166</i> , 284 ¹
Co–Pt cluster	1 M KOH	10	50	<i>J. Mater. Chem. A</i> 2018 , <i>6</i> , 20214
<i>h</i> -CoFeNi LDHs	1 M KOH	10	71	<i>Adv. Mater.</i> 2020 , <i>32</i> , 2006784
Ce–CoP	1 M KOH	10	92	<i>Nano Energy</i> 2017 , <i>38</i> , 290
Se–NiSe ₂	1 M KOH	10	133	<i>J. Mater. Sci. Technol.</i> 2022 , <i>118</i> , 136
Co/Se–MoS ₂ –NF	1 M KOH	10	104	<i>Nat. Commun.</i> 2020 , <i>11</i> , 1853
NF@NiFe LDH/CeO _x	1 M KOH	10	154	<i>ACS Appl. Mater. Interfaces</i> 2018 , <i>10</i> , 35145
P–Co ₃ O ₄	1 M KOH	10	120	<i>Energy Environ. Sci.</i> 2017 , <i>10</i> , 2563
Mn–FePSe ₃	1 M KOH	10	102	This work

